PHYSICAL REVIEW D **80,** 103521 (2009)

Are we seeing the beginnings of inflation?

Cosmin Ilie,[1,*] Tirthabir Biswas,[2,†] and Katherine Freese[1,‡]

[1]*Michigan Center for Theoretical Physics, Physics Department, University of Michigan, Ann Arbor, Michigan 48109, USA*

[2]*Department of Physics, Pennsylvania State University, University Park, Pennsylvania, 16802-6300, USA*

(Received 11 August 2009; published 30 November 2009)

Phantom cosmology provides a unique opportunity to ''connect'' the phantom-driven (low energy meV scale) dark energy phase to the (high energy grand unified theory scale) inflationary era. This is possible because the energy density increases in phantom cosmology. We present a concrete model where the energy density, but not the scale factor, cycles through phases of standard radiation/matter domination followed by dark energy/inflationary phases, and the pattern repeating itself. An interesting feature of the model is that once we include interactions between the ''phantom fluid'' and ordinary matter, the big-rip singularity is avoided with the phantom phase naturally giving way to a near exponential inflationary expansion.

DOI: 10.1103/PhysRevD.80.103521 PACS numbers: 98.80.Cq, 04.50.−h, 11.27.+d

I. INTRODUCTION

The current accelerated expansion of the Universe is usually explained by invoking a dark energy (DE) component[1] which today comprises more than 70% of the total energy in the Universe (for reviews, see [4–6]). The case of a pure cosmological constant, with $w_\Lambda \equiv p_\Lambda/\rho_\Lambda = -1$ marks the divide to the ''phantom'' realm. Phantom dark energy models are described by systems with

$$w_p = \frac{p_p}{\rho_p} < -1 \tag{1}$$

and have the intriguing feature that the energy density in the Universe increases with expansion,

$$\rho_p \sim a^{-3(1+w_p)}. \tag{2}$$

Hence a Universe with low ∼meV scale accelerated expansion can eventually reach energy scales close to the grand unified theory (GUT) scale, for instance. For some examples of cosmological scenarios using phantom energy, see [7,8]. The question that we want to ask is whether it is possible to exploit this feature of phantom cosmology and turn the dark energy driven acceleration into a GUT scale inflationary phase.[2] The idea then would be to construct a cyclic model where dark energy/inflationary phases are interspersed with decelerating radiation/matter phases.

Several problems immediately appear. First, unless the equation of state for the phantom phase, w_p, is extremely close to -1, the phantom acceleration will be much faster than the de Sitter expansion, and cannot be reconciled with data. Density perturbations produced during a phantom phase will give rise to a blue spectrum, and consistency with the current WMAP 5-yr data at the 2σ level with tensor modes included [10] require $-1 > w_p > -1.01$. Second, it is well known that phantom cosmology typically ends in a big-rip singularity, rather than the standard radiation phase which follows inflation. Remarkably, we find that both of these problems can be addressed when we include interactions between the ''phantom fluid'' and some hidden sector matter. Such interactions ameliorate the phantom acceleration phase to an asymptotic de Sitter type expansion, once the phantom energy density reaches a critical value. It is easy to arrange this transition to occur around the GUT scale, which is appropriate for inflationary cosmology. This also automatically avoids the big-rip singularity as the space-time now approaches a de Sitter universe. The density perturbations can have a variety of possibilities, allowing for agreement with observations [10]. Moreover, in our scenario the Universe transitions to an asymptotic de Sitter phase independent of the value of ω_p, and thus avoids having to fine-tune w_p very close to -1. As an additional advantage over the usual slow-roll inflationary scenario, in our phantom-driven inflationary model one does not have to tune the flatness of the potential usually necessary to obtain the large number of e-foldings and near scale-invariant spectrum. In addition, the hierarchy between the ∼meV dark energy scale and the GUT inflation scale can be reexpressed in terms of four parameters that take values of $\mathcal{O}(1)$ to $\mathcal{O}(10^2)$. We cannot however address the ''coincidence'' problem in our picture. Finally, there is the question of how to construct a theoretically self-consistent model of phantom energy. We will comment on this problem shortly.

Before delving into the details of our specific realization of the ''phantom cyclic model,'' let us outline the basic picture by considering just a simple two fluid model, phantom matter (ρ_p) + radiation(ρ_r). The cosmology we want to realize is the following: although the scale factor

*cilie@umich.edu

†tbiswas@gravity.psu.edu

‡ktfreese@umich.edu

[1]For alternative approaches which try to avoid dark energy by invoking large scale inhomogeneities, see, for instance, [1–3].

[2]For a brief list of papers that propose various mechanisms of connecting the current accelerated expansion to inflation see [9]

always increases monotonically with time, the energy density "cycles," at least approximately. Each cycle is divided into two different phases: (a) Radiation dominated phase, which starts at an energy density $\rho_r = \lambda_{\rm max}^4$. As the Universe expands radiation gets diluted, the Hubble parameter decreases and reaches a minimum when $\rho_r = \rho_p = \lambda_{\rm min}^4$. From here on we enter (b) the phantom energy dominated phase. In realistic cosmology the radiation phase should give way to matter domination at energy densities $\sim(10\ {\rm eV})^4$, before giving way to phantom domination, but for simplicity we are going to ignore this slight complication. Thus for a typical scenario which would be consistent with the dark energy and inflationary paradigm, $\lambda_{\rm max} \sim 10^{15}\ {\rm GeV} \sim 10^{-3} M_p$ or the GUT scale, and $\lambda_{\rm min} \sim {\rm meV} \sim 10^{-30} M_p$ corresponding to the scale of current energy density. Now, in the phantom phase, as the Universe expands the energy density increases, and so does the Hubble rate. Initially, depending upon how negative the phantom equation of state parameter, ω_p, is this increase in energy density can be quite fast. However, in our model we will see that once the energy density reaches close to a critical scale $\lambda_{\rm max}$, which is determined by the interactions between the hidden and ordinary matter sector, the energy density and the Hubble parameter asymptote to a constant giving rise to a near exponential expansion. This inflationary phase can end via the reheating mechanism described in Secs. III and IV after which we enter the radiation dominated era of the next cycle.

A similar idea to the one in this paper has previously been presented by [11] who dubbed this model "the eternally expanding cyclic universe." They too (in their Sec. 4c) suggested an alternating increasing/decreasing energy density. However the theory behind their model is quite different from ours, and consequently their predictions for resultant density perturbations are different as well.[3] One major problem of all phantom type models is the vacuum stability due to the null energy condition violation. [11] examine a consistent way to solve this problem, based on a deformation of the ghost condensate model of Arkani-Hamed *et al.* [12].

Although the interactions between phantom fluid and ordinary matter can lead to an inflationary space-time, we are still left with a graceful exit problem, or how to ensure that the Universe enters the standard radiation dominated era. Depending upon the specific model, different "reheating mechanisms" may be able to trigger such a transition. We focus on a model where the phantom fluid consists of a ghostlike scalar field coupled to some hidden matter sector. Such a fluid closely resembles the interacting DE-dark matter models [13–16] except that the scalar field instead of being an ordinary quintessence field, has negative kinetic energy like a ghost. Although field theory with ghosts is plagued with problems of unitarity/instability [17], recent developments attempting to address these problems include progress in nonlocal [18] and Lee-Wick [19] higher derivative models; see also [11,20]. As we will see, in our model the transition from phantom to radiation phase and vice versa is achieved partly by suitably choosing the interaction strength between the scalar field and the hidden matter sector, and partly due to the presence of interactions between the hidden and ordinary matter sector. (There is no direct coupling between the ghost field and ordinary matter.)

As emphasized before, the main reason why the cosmology described above can replace the standard inflationary paradigm is because in the phantom phase the energy density increases even though the Universe continues to expand. Thus after the usual dilution in a radiation dominated phase, the phantom phase followed by reheating ensures that the Universe again becomes hot and therefore can reproduce the successes of the big bang model, such as big bang nucleosynthesis and cosmic microwave background (CMB) radiation. There is another essential similarity between our scenario and the inflationary paradigm. The essential reason why inflation solves the standard cosmological puzzles is because our observable universe (of radius $\sim H_0^{-1}$) can originate from a very tiny region at the beginning of inflation. Something very similar happens in our model as well, the Universe expands by a huge factor in every cycle. In our model the number of e-foldings in the radiation and the phantom phase is given by

$$\mathcal{N}_{\rm rad} \sim \ln\left(\frac{\lambda_{\rm max}}{\lambda_{\rm min}}\right) \quad \text{and} \quad \mathcal{N}_{\rm phan} \sim \frac{-4}{3(1+\omega_p)} \ln\left(\frac{\lambda_{\rm max}}{\lambda_{\rm min}}\right). \tag{3}$$

In order to have a successful GUT scale inflationary paradigm we need $\mathcal{N}_{\rm inf} \gtrsim 60$. Thus one gets

$$\begin{aligned}\mathcal{N}_{\rm tot} &= \mathcal{N}_{\rm phan} + \mathcal{N}_{\rm rad} + \mathcal{N}_{\rm inf} \\ &\sim \left(1 - \frac{4}{3(1+\omega_p)}\right) \ln\left(\frac{\lambda_{\rm max}}{\lambda_{\rm min}}\right) + \mathcal{N}_{\rm inf}.\end{aligned} \tag{4}$$

Just to get an idea, if we take $\lambda_{\rm min} \sim {\rm meV}$, $\lambda_{\rm max} \sim 10^{15}$ GeV, $\omega_p \sim -1.3$, and $\mathcal{N}_{\rm inf} \sim 60$, we get $\mathcal{N}_{\rm tot} \sim 400$. What this means is that only a very, very tiny portion (for the chosen example, e^{-400}th) of our observable universe will ultimately grow to become the observable universe in the next cycle at the same energy density scale. Another essential similarity between the standard inflationary scenario and our phantom based model, is the production of a huge amount of entropy in every cycle. Even in a "cyclic" scenario if one wants to address the usual cosmological puzzles, such as flatness, homogeneity, etc., as well as produce cosmological perturbations with the correct amplitude required for galaxy formation, entropy production seems to be an inevitable requirement

[3]They always predict a negative, even if extremely small, tilt of the spectral index while our model will allow a variety of possibilities (as discussed in later sections of this paper).

[21]. Like in inflation, in our scenario a huge amount of entropy is produced during reheating when most of the phantom energy is converted into radiation. This is essential to ensuring the cyclicity of energy density even though the scale factor of the Universe is monotonically increasing.[4]

It is worth mentioning that in most cyclic models that proposed the scale factor $a(t)$ have a contracting-expanding behavior, where both a bounce, near the big bang, and a turnaround, when the scale factor becomes large are needed. A brief and incomplete compilation of some of the papers that have proposed cyclic cosmologies can be found in [8,23]. Such cosmologies provide natural solutions to the flatness and horizon problems of the standard big bang scenario. Some variants also avoid the issue of initial conditions, provided entropy produced during one cycle is not transferred to the next. In this case the cycles will not grow, i.e., become larger (Tolman's argument [24]) from one to the next, so we can no longer define a beginning of the Universe. For instance the authors of [25] developed an ekpyrotic inspired cyclical model as an alternative to inflation, where a phase of slow contraction before the bang is responsible for generating a nearly scale-invariant spectrum of perturbations that seed the large scale structure formation. In contrast, the standard inflationary scenario assumes a short phase that occurs after the big bang when the Universe is rapidly expanding and nearly scale-invariant perturbations are generated.

The paper is organized as follows. In Sec. II we present our model of phantom fluid and discuss the cosmology relevant for dark energy. In Sec. III, we discuss how including interactions can lead to an inflationary spacetime along with partially reheating the Universe. In Sec. IV we provide a specific example where transitions from the phantom-inflation phase to radiation and vice versa can be orchestrated giving us a cyclic model of the Universe. In Sec. V we discuss the different observational constraints coming from inflation, big bang nucleosynthesis (BBN), and dark energy experiments. Finally, we conclude with a summary of the scenario presented and issues that need to be addressed further.

II. PHANTOM DARK ENERGY

The purpose of this section is to implement a model for the phantom component that would drive the superaccelerated expansion. For now we will not include regular matter nor radiation, but rather focus solely on the components necessary to obtain a phantom phase. One can possibly implement the cosmology sketched before in many different ways. Here we are going to realize the above picture using a ghostlike scalar field (with negative kinetic energy) ϕ coupled to a hidden matter sector which we denote by index "h." There are two equivalent approaches to describe this type of coupling. One starting from an action, where we allow for a direct coupling term between the hidden sector and the scalar field. The second approach is to consider two fluids that can exchange energy while maintaining the conservation of the total stress-energy tensor, as required by diffeomorphism invariance, although the individual stress-energy tensors are not conserved.

Our system will be described by the following action:

$$S = \int d^4x\sqrt{-g}\left[M_p^2\frac{R}{2} + \frac{(\nabla\phi)^2}{2} + C(\phi)\mathcal{L}_h\right], \quad (5)$$

where $\mathcal{L}_h$ does not depend on ϕ, being the action describing a perfect barotropic fluid. Here we work with a spatially flat Friedmann-Robertson-Walker metric with signature $(-,+++)$. Notice that the kinetic term for the scalar field comes with the "wrong" sign, as appropriate for a ghost. In the phantom dominated phase, described here, the Hubble equation derived from the action above looks like

$$H^2 = \frac{1}{3M_p^2}(\rho_\phi + \rho_h) = \frac{1}{3M_p^2}\left[-\frac{\dot\phi^2}{2} + C(\phi)\tilde\rho_h\right], \quad (6)$$

where we have assumed the field ϕ to be homogenous. Here a dot represents the derivative with respect to cosmic time, t and $\tilde\rho_h$ denotes the bare energy density of the hidden sector, which is ϕ independent. We will assume that it behaves like a perfect barotropic fluid, satisfying the continuity equation:

$$\dot{\tilde\rho}_h + 3H(\tilde\rho_h + \tilde p_h) = 0 \quad (7)$$

with an equation of state

$$\tilde p_h = \omega\tilde\rho_h. \quad (8)$$

One can also include a potential for the scalar field, and its effects are discussed briefly in Appendix A, but for the purpose of illustration we are going to set it to zero.

The interaction that we are going to consider between the hidden matter sector and ϕ is going to be very similar to the interactions considered in coupled quintessence (or interacting DE-dark matter) models [13–15]. From the action in Eq. (5) we get two additional equations of motion:

$$\ddot\phi + 3H\dot\phi = 2\rho_h\mu(\phi)/M_p \quad (9)$$

$$\dot\rho_h + 3H(1+\omega)\rho_h = 2\rho_h\dot\phi\mu(\phi)/M_p, \quad (10)$$

where we have defined

$$\mu(\phi) \equiv \frac{1}{C}\frac{dC}{d\phi}, \quad (11)$$

and we are going to assume hence forth that $\mu(\phi)$ always remains positive. As one can see, both the Klein-Gordon equation for ϕ and the continuity equation for the hidden matter sector ρ_h are augmented by interaction terms in the

[4]It may be possible to embed the scenario in phantom cyclic models [8,22] with actual phases of contraction, but we are not going to explore this possibility here.

right-hand side of Eqs. (9) and (10). Although μ in general depends on ϕ, to understand the phantom phase let us consider a constant μ to begin with. It is easy to check that the above interaction is consistent with the conservation of the total energy momentum tensor:

$$\dot{\rho}_{\rm tot} + 3H(\rho_{\rm tot} + p_{\rm tot}) = 0, \tag{12}$$

where $\rho_{\rm tot} \equiv \rho_h + \rho_\phi$. To see this we remind the readers that the Klein-Gordon equation can be recast as

$$\frac{d}{dt}\left[-\frac{\dot{\phi}^2}{2}\right] - 3H\dot{\phi}^2 = -2\rho_h\mu\dot{\phi} \Rightarrow \dot{\rho}_\phi + 3H(\rho_\phi + p_\phi) = -2\rho_\phi\dot{\phi}\mu(\phi), \tag{13}$$

since the energy density and pressure for a phantom scalar field are given by

$$\rho_\phi = p_\phi = K = -\frac{\dot{\phi}^2}{2}. \tag{14}$$

Thus the source terms in the individual conservation equations (10) and (13) cancel each other.

One can solve the hidden matter continuity equation exactly to find

$$\rho_h = \rho_{h0}C(\phi)\left(\frac{a}{a_0}\right)^{-3(1+\omega)}, \tag{15}$$

where we have chosen the convention that at $a = a_0$, $C(\phi) = 1$, and $\rho_h = \rho_{h0}$. The $a^{-3(1+\omega)}$ dependence reflects the usual dilution of the energy density of an ideal fluid with expansion. Depending upon the scale of energy density relative to the mass of the hidden matter particles, they can either behave as nonrelativistic matter ($\omega = 0$) or like a relativistic species ($\omega = 1/3$).[5] We will for the most part consider a light degree of freedom, so that approximately it behaves like radiation.

For the special case when μ is a constant, the coupling function is given by

$$C(\phi) = e^{2\mu(\phi-\phi_0)/M_p}. \tag{16}$$

Now, coming back to the evolution equations, we only need to solve the Hubble equation (6) and the Klein-Gordon equation, the latter simplifying to

$$\ddot{\phi} + 3H\dot{\phi} = \frac{2\mu\rho_{h0}}{M_p}e^{2\mu(\phi-\phi_0)/M_p}\left(\frac{a}{a_0}\right)^{-3(1+\omega)} \equiv V'_{\rm eff}(\phi). \tag{17}$$

It is as if the phantom scalar field is evolving under the influence of an "effective potential" given by

$$V_{\rm eff}(\phi) = \rho_h(\phi) = \rho_{h0}e^{2\mu(\phi-\phi_0)/M_p}\left(\frac{a}{a_0}\right)^{-3(1+\omega)}. \tag{18}$$

An important thing to note is the +ve sign appearing in front of $V'_{\rm eff}$ in Eq. (17) because ϕ is a ghost field with negative kinetic energy. It is clear now that because of the peculiar properties of the phantom field, ϕ actually rolls up the effective potential $e^{2\mu\phi/M_p}$.

We have the following late time attractor power-law solutions:

$$a(t) - a_0\left(\frac{t}{t_0}\right)^n \quad \text{and} \quad \phi = \phi_0 + pM_p\ln\left(\frac{t}{t_0}\right) \Longleftrightarrow e^{\phi/M_p} = e^{\phi_0/M_p}\left(\frac{t}{t_0}\right)^p, \tag{19}$$

with

$$n = -\frac{1-\omega}{4\mu^2 - 3/2(1-\omega^2)} \quad \text{and} \quad p = -\frac{4\mu}{4\mu^2 - 3/2(1-\omega^2)}. \tag{20}$$

We have verified (see Appendix A) that these late time attractors are indeed stable.[6]

In this phase the scalar field and the hidden matter are tightly coupled and evolve as a single fluid with an effective equation of state parameter

$$\omega_p \equiv p_\phi + \frac{p_h}{\rho_\phi + \rho_h} \rightarrow -\frac{8}{3}\frac{\mu^2}{(1-\omega)} + \omega. \tag{21}$$

The asymptotic value is attained during the late time attractor phase. In the phantom phase, expansion of the scale factor is controlled by ω_p, since $a(t) \sim t^{2/[3(1+\omega_p)]}$. These are analogues to the coupled quintessence solutions [13–15]. A detailed derivation of all results presented in this section can be found in Appendix A. The crucial thing to note is that as long as

$$\mu^2 > \tfrac{3}{8}(1-\omega^2) \tag{22}$$

we have a phantom phase, i.e., $\omega_p < -1$. In particular for $\omega = 1/3$ the last condition gives a constraint on μ,

$$\mu > \frac{1}{\sqrt{3}}. \tag{23}$$

In passing we also note that in this phase most of the energy density is actually stored in the hidden sector; one can

[5] In this context we note that we have a choice in how we interpret the augmentation of the energy density with the growth of ϕ. One can either think of this growth as simply the increase in mass of the hidden matter particles if the mass depends on ϕ, or creation of the hidden matter particles through its interactions with ϕ, or a combination of the two. To keep things simple we are going to assume that the mass of the hidden matter particles remains a constant, but its number density increases.

[6] We have not investigated whether these solutions suffer from any hydrodynamic instabilities of the nature found in some interacting quintessence models [13], and we leave this for a future exercise.

check that the tracking ratio between scalar field and the hidden matter density is given by

$$-\frac{\rho_\phi}{\rho_h} = -\frac{K}{\rho_h} = \frac{8\mu^2}{3(1-\omega)^2 + 8\mu^2} < 1. \tag{24}$$

One can also evaluate the amount by which ϕ evolves during this phase. A straightforward calculation gives us

$$\Delta\phi_p = \frac{2}{\mu}\left[1 - \frac{4}{3(1+\omega)}\right]\ln\left(\frac{\lambda_{\max}}{\lambda_{\min}}\right). \tag{25}$$

Here $\lambda_{\min}$ and $\lambda_{\max}$ represent the energy scale at which the phantom phase begins and ends, respectively.

In summary, in this section we have found under what conditions a phantom phase could be described by a stable late time attractor for ghostlike fields coupled exponentially to a perfect fluid. The purely phantom sector we have studied in this section is problematic as an inflationary model. For example, for a constant (purely) phantom equation of state $\omega_p < -1$, typically one would obtain a blue spectrum [see Eq. (59)] which would be inconsistent with the WMAP data. This conclusion is of course valid with the assumption that primordial perturbations are generated mostly during the phantom phase. Thus unless μ is fine-tuned to be very close to the critical value (which gives rise to $\omega_p = -1$), we will not be able to reproduce the inflationary near scale-invariant spectrum. Thus far we have considered the phantom sector alone; in the next section we include interactions with the standard model which ameliorate some of the problems of a phantom sector alone.

III. "PARTIAL REHEATING" AND LATE TIME DE SITTER PHASE

In the previous section we realized the phantom phase through an interacting phantom scalar field and hidden matter sector. In the absence of any new physics this phase is going to last until the big-rip singularity, as is well known in phantom cosmology. In order for the next cycle to begin we need to first find a "reheating" mechanism which converts most of the phantom energy density to radiation.

What we find, quite remarkably, is that once we include interaction between the hidden matter sector and standard model particles (namely we allow the hidden sector particles to be converted to light degrees of freedom of the standard model), which generically exist, it naturally ameliorates the phantomlike acceleration to a near exponential inflationary expansion.

As we will see, such interactions begin the process of reheating the Universe by producing a radiation bath. Unfortunately the interactions do not provide us with a graceful exit from the inflationary phase, but we will discuss how this issue can also be addressed in the next section.

To understand how interactions affect the cosmological evolution we will use Boltzmann equations in the following form:

$$\dot{\rho}_h + 3H(1+\omega)\rho_h = -\rho_h\Gamma + 2\rho_h\dot{\phi}\frac{\mu}{M_p}, \tag{26}$$

$$\ddot{\phi} + 3H\dot{\phi} = 2\rho_h\frac{\mu}{M_p}, \tag{27}$$

$$\dot{\rho}_\gamma + 4H\rho_\gamma = \rho_h\Gamma, \tag{28}$$

along with the Hubble equation

$$H^2 = \frac{1}{3M_p^2}\left(\rho_h - \frac{\dot{\phi}^2}{2} + \rho_\gamma\right). \tag{29}$$

Here by ρ_γ we denote the energy density of all the light degrees of freedom which do not couple directly to the phantom field, and Γ is the annihilation rate of the hidden matter particles into all these other light degrees of freedom. We have ignored the inverse process of creation of the hidden matter particles from the rest of the matter under the assumption that the equilibrium density of the hidden matter sector is small compared to normal radiation. The annihilation rate, per hidden sector particle, is given in general by

$$\Gamma_{h\bar{h}\to\gamma\gamma} = n_h < \sigma|v| >_{h\bar{h}\to\gamma\gamma}, \tag{30}$$

where $<\sigma|v|>$ is the average over all initial and final states of the differential cross section times the relative velocities of the annihilating particles. Usually one is used to consider the opposite process while trying to determine when a given species freezes out. In the latter case since the photons are in thermal equilibrium, one can use thermal distribution functions to compute the "thermally averaged" $<\sigma|v|>$. However, in our case in order to compute $<\sigma|v|>$ we would need information regarding the velocity distribution of the produced hidden particles from ϕ. In the absence of any microphysical theory of such an interaction, for the purpose of illustration, here we are simply going to assume that $<\sigma|v|>$ is a constant set by the details of the interaction, so that the interaction rate per hidden sector particle is given by

$$\Gamma = \frac{\rho_h}{m^3}. \tag{31}$$

Here m is an energy scale we introduce as a free parameter. More generally one expects Γ to go as some power law, $\Gamma \sim \rho_h^\lambda$, the power being determined by the microphysics, but most of our results and conclusions should hold qualitatively as long as $\lambda > 1$.

It is easy to check that the above set of equations (26)–(28) has an asymptotic de Sitter late time attractor solution where all the energy densities and the Hubble parameter tend to a constant. Defining the following dimensionless variables,

$$\xi \equiv \frac{\rho_h}{M_p^2 H^2} \quad \text{and} \quad \eta \equiv \frac{\Gamma}{H} = \frac{\rho_h}{m^3 H},$$

we have

$$\xi \to \frac{27\omega - 9 + 3\sqrt{9(3\omega-1)^2 + 192\mu^2}}{8\mu^2}, \tag{32}$$

$$\eta \to \frac{3\omega - 9}{2} + \frac{1}{2}\sqrt{9(3\omega-1)^2 + 192\mu^2}, \tag{33}$$

$$\dot{\phi} = \frac{2\rho_h \mu}{3H} \to \frac{2\mu m^3 \eta}{3M_p}, \tag{34}$$

$$\rho_\gamma = \frac{\rho_h^2}{4Hm^3} \to \frac{m^6 \eta^3}{4M_p^2 \xi}. \tag{35}$$

As a consistency check we have evolved Eqs. (26)–(28) numerically, see Fig. 1, and have verified that the asymptotic values are exactly the ones predicted by the above set of equations. Let us make a few observations. Since we are specializing to $\omega = 1/3$, let us look at the asymptotic value of the energy densities in this case:

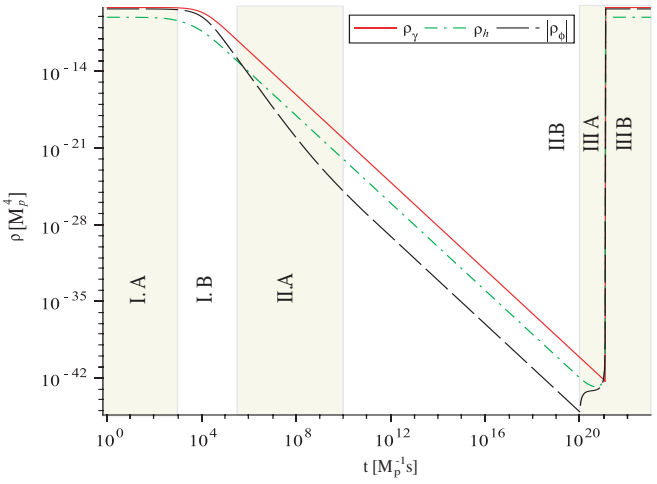

FIG. 1 (color online). Numerical solutions for the energy densities as we complete a cycle from a de Sitter phase back to it. Here we have chosen $\omega = \frac{1}{3}$, $\mu_p = 5$, $\mu_r = .1$, $m = 10^{-2} M_p$ and we have set M_p to one. Note the six distinct phases: I.A and I.B corresponding to reheating; II.A and II.B corresponding to a radiation dominated universe; III.A and III.B corresponding to the phantom and dS phase, respectively. In order to make all phases clearly distinct we set the minimum energy density at around $10^{-45} M_p^4$ instead of the realistic meV^4.

$$\rho_\gamma = \frac{16\sqrt{3}\mu m^6}{9M_p^2}(\sqrt{3}\mu - 1)^3,$$
$$\rho_h = \frac{16\sqrt{3}\mu m^6}{9M_p^2}(\sqrt{3}\mu - 1)^2, \tag{36}$$
$$\rho_\phi = -\frac{32\mu^2 m^6}{9M_p^2}(\sqrt{3}\mu - 1)^2.$$

Note that the solutions above are consistent only if $\mu > \frac{1}{\sqrt{3}}$, but we know this is also a requirement for the existence of a phantom phase [see Eq. (23)] which will eventually settle to this de Sitter attractor. In particular, we find that for $\mu \gg 1$, which is the case we will eventually be focusing on, radiation dominates over the hidden sector:

$$\mathcal{R} \equiv \frac{\rho_h}{\rho_\gamma} \approx \frac{1}{4\sqrt{3}\mu} \ll 1 \quad \text{for } \mu \gg 1. \tag{37}$$

In other words, as μ increases, the conversion from hidden matter to radiation becomes more efficient, and, in particular, radiation can easily dominate the total energy density. However, this does not mean that we can enter into the usual radiation dominated epoch because the equation of state for all the energy densities essentially approach $\omega_p = -1$, as all the energy densities approach the constant asymptotic values in Eq. (36). Physically, the energy density that the phantom field was pumping into the hidden matter sector is now transferred to radiation through its interaction with the hidden sector, in such a way that we approach a de Sitter universe. This phase however is good for inflationary cosmology as fluctuations produced during this de Sitter phase are expected to give rise to a near scale-invariant spectrum (allowed, although not favored, by the WMAP data). In order for the amplitude of the fluctuations to be consistent with observations we require

$$\rho_\gamma \approx 10^{-12} M_p^4 \Rightarrow m \sim 10^{-2} M_p. \tag{38}$$

We will return to the constraint coming from the number of e-foldings required for a successful inflationary paradigm later.

In this section we have found that the big-rip singularity could be avoided in this model if the hidden sector particles are converted to light degrees of freedom of the standard model. As the energy densities approach their asymptotic values, the Universe will enter in a de Sitter phase. Of the three components, radiation is dominant, yet the Universe is inflating. This is due to the interplay between the coupling of the hidden sector to the phantom field and light degrees of freedom of the standard model which leads to a state where all the energy densities approach a constant value.

IV. TRANSITION TO RADIATION AND CYCLICITY

In the above section we saw that interactions between hidden matter and radiation can ameliorate the phantom like acceleration to exponential inflation but cannot provide a graceful exit from the de Sitter inflationary phase. So far we have assumed that μ remains a constant leading to an exponential coupling between the hidden sector and the phantom field as in Eq. (16). If $\mu(\phi)$ is not a constant, a graceful exit becomes possible. Here we explore the case when $\mu(\phi)$ is periodic. For simplicity we will just assume a step function for $\mu(\phi)$, where

$$\mu = \mu_p \gg 1 \quad \text{for } 0 < \phi < \phi_R \tag{39}$$

$$\mu = \mu_r \ll 1 \quad \text{for } \phi_R < \phi < \phi_0 \tag{40}$$

and then the pattern repeats itself. The first phase, when $\mu \gg 1$, reproduces the phantom phase discussed in the previous section, leading eventually to the late time de Sitter-like attractor evolution. However, now this inflationary phase ends once ϕ reaches the transition value ϕ_R. We are also going to assume that $\omega = 1/3$ in this scenario. We remind the readers that ω describes the hidden sector, as in Eq. (8). As we will see shortly, the periodicity in μ will ensure that we enter the standard radiation dominated era which lasts until ϕ rolls to ϕ_0.

The evolution of the Universe during one cycle can be described in our model using three phases, as indicated in Fig. 1. Phase I provides the reheating from inflationary expansion. Phase II describes a standard radiation dominated era. Then a short phantom phase III.A ensues, during which the energy is driven from the meV to the GUT scale. This is followed by a de Sitter inflationary phase III.B. After one such cycle is complete, the next one begins, again cycling through phases I, II, III.A, and III.B successively.

A. Phase I: Reheating

The reheating process is most easily understood when $\mu_r = 0$ [defined in Eq. (40)], so let us first focus on this simple case. As we discussed in the previous section, as long as μ is large, although radiation is the dominant energy density, the de Sitter phase continues. However, if and when μ sharply falls to zero, the phantom phase indeed ends. Two things happen. First, since initially Γ is comparable to H, as it can be seen from Eq. (33), there is rapid conversion of the hidden matter to radiation, but the hidden matter sector now no longer gets replenished by the scalar field. Second, the driving term in the right-hand side of the Klein-Gordon equation for the phantom scalar field (9) is now absent and as a result ϕ slows due to Hubble damping, $\rho_\phi \sim a^{-6}$, and eventually comes to a halt. At the beginning of the reheating phase the energy densities of radiation, hidden matter, and ϕ are approximately given by the asymptotic values of the late time de Sitter phase (36). As we had pointed out before, for $\mu \gg 1$ radiation is the dominant energy density component in this asymptotic phase. The reheating phase further ensures that radiation continues to dominate the energy density. If one tracks the ratio of the energy densities between hidden matter and radiation, $\mathcal{R}$, then it starts with the asymptotic value given by Eq. (37), decreases rapidly during conversion, and then approaches a constant, $\mathcal{R}_{\min}$, once the conversion ends. Note, since ϕ slows down, ρ_h redshifts almost as radiation and therefore maintains an approximately constant tracking ratio approaching $\mathcal{R}_{\min}$. In Appendix B we calculated this asymptotic ratio to be

$$\mathcal{R}_{\min} \approx \frac{1}{6}\frac{\sqrt{3}}{\mu_p^2} \quad \text{for } \mu_r = 0, \qquad \mu_p \gg 1. \tag{41}$$

Qualitatively, it turns out that one can distinguish two different regimes in the reheating phase depicted in Fig. 1 as phases I.A and I.B. Numerically we found that even after $\mu \to 0$, it takes a while for the radiation energy density to start decreasing substantially. The reason is somewhat technical and the reader is referred to Appendix B for details. Intuitively, the main reason is that initially the Hubble damping of radiation is compensated by the hidden matter decays into radiation, $4H\rho_\gamma \sim \rho_h\Gamma$. Since radiation is the dominant component of the energy density, this in turn leads to H being approximately constant, as can be seen in phase I.A of Fig. 1. Once ρ_h decreases appreciably so that $\rho_h\Gamma \ll 4H\rho_\gamma$, the radiation energy density starts to decrease appreciably and therefore so does the Hubble rate. This is depicted in phase I.B of Fig. 1. At some point, the conversion from hidden matter to radiation effectively stops, marking the end of the reheating phase.

Although the above discussion has been for $\mu_r = 0$, we note that for a nonzero but small μ_r, the reheating phases (I.A, I.B) follow basically the same pattern as in the $\mu_r = 0$ case. The asymptotic tracking ratio[7] between hidden matter and radiation receives a slight correction:

$$\mathcal{R}_{\min} \sim \frac{1}{18}\frac{\sqrt{3}(3 + 8\mu_r)}{\mu_p^2} \quad \text{for } \mu_r \ll 1, \qquad \mu_p \gg 1. \tag{42}$$

We have checked this numerically, and some of the more technical details are discussed in Appendix B.

B. Phase II: "Standard" radiation domination

After the reheating phase, since hidden matter is no longer converted into radiation, the latter starts to evolve

[7]Unlike in the $\mu_r = 0$ case where the tracking ratio keeps decreasing and asymptotically approaches $\mathcal{R}_{\min}$, when $\mu_r \neq 0$, $\mathcal{R}_{\min}$ is actually a minimum of the tracking ratio that is attained. Since ϕ never comes to a halt, the ratio does increase from its minimum value of $\mathcal{R}_{\min}$, but this increase is very slight.

as $a(t)^{-4}$, and consequently $H \sim 1/2t$ as in the standard radiation dominated era. In the meantime ϕ continues to be Hubble damped. Once the scalar field effectively stops evolving, the hidden matter starts redshifting as radiation and thus settles down to its constant tracking ratio given in Eq. (41). In particular, one can see from (42) that for sufficiently large values of μ_p, this ratio can be quite small and easily satisfy constraints coming from BBN and CMB. BBN/CMB only constrains the abundance of the dark radiation component to be less than around 10% [26]. In Fig. 1 we refer to the phase when ϕ is being Hubble damped as phase II.A, and the subsequent radiative phase as phase II.B.

If μ_r is precisely zero, then the radiation dominated phase II.A can continue forever because ϕ will effectively come to a halt, and unless the value of ϕ_0 is fine-tuned, ϕ will never make it to the next large μ phase. As a result the next phantom phase will not begin and the cyclic picture cannot be sustained. This is why a small but nonzero value of μ_r is essential to maintaining cyclicity without having to resort to unnatural fine-tuning.

For a nonzero but small μ_r, the reheating phases (I.A, I.B) and the Hubble damping phase (II.A) follow very much the same pattern as in the $\mu_r = 0$ case, as discussed at the end of the previous section (IVA). The main difference when $\mu_r \neq 0$, as compared to the $\mu_r = 0$ case, appears in the radiative phase II.B. This is because the nonzero driving term in the Klein-Gordon (KG) equation now ensures that instead of coming to a halt, ϕ now tracks radiation. After the initial phase of Hubble damping, the driving term on the right-hand side of the KG equation catches up with the Hubble damping term. At this point the scalar field enters a phase where its energy density approximately tracks that of radiation. This can be seen in Fig. 1 where we have divided the radiation phase into two parts. II.A refers to the regime when the scalar energy density is still being Hubble damped, while phase II.B refers to the tracking phase where both the hidden matter and the scalar energy densities are tracking that of radiation.

This tracking behavior can be approximately obtained as follows: From the KG equation we have

$$3H\dot{\phi} = \frac{2\rho_h \mu_r}{M_p} \approx \frac{2\mathcal{R}_{\min}\rho_\gamma \mu_r}{M_p} \approx 6\mathcal{R}_{\min} M_p \mu_r H^2. \quad (43)$$

In the above we have ignored the $e^{2\mu_r \phi}$ dependence of ρ_h, as ϕ is rolling very slowly, and $\mu_r \ll 1$. We will perform a consistency check later. Also, we have ignored the contributions to the energy density coming from the hidden matter and the scalar field as compared to normal radiation. Again, this is justified as $\mathcal{R}_{\min} \ll 1$ and ϕ is rolling slowly. Choosing the ansatz

$$\phi = M_p p_r \ln\left(\frac{t}{t_R}\right) \Rightarrow \dot{\phi} = \frac{M_p p_r}{t}, \quad (44)$$

we find that (43) can indeed be satisfied provided

$$p_r = \mathcal{R}_{\min}\mu_r. \quad (45)$$

In the above analysis we have used the fact that in a radiation dominated universe $H \sim 1/2t$. In particular our analysis tells us that the tracking ratio between the kinetic energy of ϕ and radiation is indeed very small

$$\frac{K_\phi}{\rho_\gamma} = -\frac{2}{3}(\mu_r \mathcal{R}_{\min})^2, \quad (46)$$

justifying our earlier assumption. In the next subsection we will also see that during this phase ϕ evolves rather slowly, so that $C(\phi)$ changes only by an $\mathcal{O}(1)$ factor ensuring that the hidden matter indeed behaves as radiation to a very good approximation.

This radiation dominated tracking era lasts until ϕ reaches ϕ_0 and rolls over to the large μ region. The next phase of phantom domination, phase III.A, can now begin.

C. Cyclicity

To better understand the transition from one cycle to the next let us discuss the various phases we observe in Fig. 1, where we plot a numerical solution for the energy densities of the three components from one de Sitter inflationary phase to the next. The plot does not correspond to realistic values for $\lambda_{\max}$ or $\lambda_{\min}$, but captures all the essential features of the different phases. The plot starts (extreme left) at $t = 0$ and $\phi = \phi_R$, corresponding to the beginning of the reheating phase I.A. We have estimated in Appendix B, Eq. (B8), how long (t_{1A}) the I.A subphase lasts

$$t_{1A} = \left(\frac{3M_p^4 \xi}{m^6 \eta^3}\right)^{1/2}. \quad (47)$$

During this phase the field ϕ evolves approximately a distance of

$$\Delta\phi_{1A} = \dot{\phi}_{dS}\int_0^{t_{1A}} dt e^{-3H_{dS}t} = \frac{\dot{\phi}_{dS}}{3H_{dS}}[1 - e^{-3H_{dS}t_{1A}}]. \quad (48)$$

Above we have used

$$\dot{\phi}(t_{1A}) = \dot{\phi}_{dS} e^{-3H_{dS}t_{1A}}, \quad (49)$$

where $\dot{\phi}_{dS}$ represents the asymptotic value in the de Sitter phase, given by (34) and H_{dS} is the Hubble rate during the inflationary phase and can be solved from the definitions of ξ and η.

Phase I.A is followed by phase I.B, where although the conversion from hidden matter to radiation takes place, the Hubble rate starts to decrease appreciably as well. As soon as the conversion is no longer efficient we enter a regime, phase II.A, where radiation starts to redshift as a^{-4} marking the beginning of a standard radiation dominated era. In phase II.A radiation and the hidden sector energies ap-

proximately track each other while the field ϕ is still being Hubble damped. This phase ends when the scalar field is no longer Hubble damped and starts to track radiation as well, a phase we refer to as II.B. Next we estimate the time t_{2A}, when this transition from the Hubble damping phase II.A to tracking phase II.B occurs. It can be defined as the time when the Hubble damping term in the left-hand side of Eq. (27) is equal to the coupling term on the right-hand side (rhs). Under the assumption that we are in a radiation dominated phase and that the hidden sector energy density tracks the radiation energy density with the ratio $\mathcal{R}_{\min}$ we get

$$\frac{3\dot{\phi}(t_{2A})}{2t_{2A}} = \frac{2\mu_r}{M_p}\mathcal{R}_{\min}\rho_\gamma(t_{2A}) \Rightarrow t_{2A} = \frac{t_{1A}^3\dot{\phi}^2(t_{1A})}{M_p^2\mu_r^2\mathcal{R}_{\min}}. \tag{50}$$

This last equation can be rewritten in terms of our parameters in the following form:

$$\frac{t_{1A}}{t_{2A}} = \frac{1}{144}\frac{\mu_r^2(3+8\mu_r)^2\eta}{\xi\mu_p^6}e^{6H_{dS}t_{1A}}. \tag{51}$$

With $\omega = 1/3$ and in the limit $\mu_p \gg 1$ the exponent $6H_{dS}t_{1A}$ becomes $\sqrt{3}$, so we see, as expected, that $t_{2A} \gg t_{1A}$.

We can compute the distance the field ϕ evolves during phases I.B and II.A since the Hubble friction term is dominant during this time.

$$\Delta\phi_{1B+2A} = \int_{t_{1A}}^{t_{2A}} dt\dot{\phi} = 2\dot{\phi}(t_{1A})t_{1A}\left(1-\sqrt{\frac{t_{1A}}{t_{2A}}}\right) \approx \frac{4\mu_p}{\sqrt{3}}\sqrt{\frac{\xi}{\eta}}M_p e^{-(\sqrt{3}/2)}. \tag{52}$$

In the next phase, II.B, as one can see from the plot, all the energy components are tracking each other. Since this phase will lasts until almost "today" and it began at t_{2A} we have

$$\frac{\Delta\phi_{2B}}{M_p} \approx 2\mathcal{R}_{\min}\mu_r \ln\left(\frac{(\rho_\gamma(t_{2A}))^{1/4}}{meV}\right) \approx 120\mathcal{R}_{\min}\mu_r, \tag{53}$$

where $\Delta\phi_{2B}$ is the distance the scalar field evolves during phase II.B. In particular we note that this means

$$e^{\mu_r\Delta\phi_{2B}/M_p} \approx e^{120\mathcal{R}_{\min}\mu_r^2}. \tag{54}$$

Since $\mathcal{R}_{\min}$ is a small number, for sufficiently small values of μ_r it is easy to see that the exponential will only contribute to an $\mathcal{O}(1)$ factor to the energy density of the hidden matter sector. In other words unlike the $\mu_r = 0$ case, although the ratio $\mathcal{R}$ does not monotonically decrease during the radiation phase, but rather starts to increase as ϕ evolves, this increase is very slow. This justifies our earlier assumption of hidden matter approximately behaving as radiation.

The advantage of having a nonzero μ_r is that it keeps the scalar field rolling, albeit slowly, ensuring passage to the next phantom phase when ϕ reaches ϕ_0. Therefore, no fine-tuning is involved in restarting the phantom era. To see this, observe that

$$\Delta\phi_{2B} = (\phi_0 - \phi_R) - (\Delta\phi_{1A} + \Delta\phi_{1B+2A}) \tag{55}$$

and crucially for realistic values of the parameters the three different $\Delta\phi$'s are of the same order of magnitude, as we shall see in Sec. V. If for instance, it turned out that $\Delta\phi_{2B} \ll \Delta\phi_{1A} + \Delta\phi_{1B+2A}$, that would have meant fine-tuning the range $\phi_0 - \phi_R$ to cancel $\Delta\phi_{1A} + \Delta\phi_{1B+2A}$ to very high precision. In fact, this is what one has to do as $\mu_r \to 0$.

A related nice feature of the model is that the exponential hierarchy between the scales of inflation and dark energy is rather easy to arrange. To see this let us try to obtain $\lambda_{\min}$ in terms of $\phi_0 - \phi_R$. By rearranging Eq. (53) one finds that the energy density at the beginning of the phantom phase is given by[8]

$$\lambda_{\min} \sim \lambda_{\max}\exp\left(-\frac{\Delta\phi_{2B}}{2\mathcal{R}_{\min}\mu_r M_p}\right) \sim 10^{-3}M_p\exp\left(-\frac{\phi_0 - \phi_R - \Delta\phi_{1A} - \Delta\phi_{1B+2A}}{2\mathcal{R}_{\min}\mu_r M_p}\right). \tag{56}$$

Since $\mathcal{R}_{\min}$, μ_r are small numbers as compared to $\Delta\phi/M_p$'s, it is easy to arrange the exponential suppression of ρ_0 as compared to the GUT scale. Conversely, we can reformulate the "smallness" problem associated with dark energy in terms of four parameters: μ_p, μ_r, ϕ_R, ϕ_0, which as we shall see shortly have values that range from $\mathcal{O}(1)$ to $\mathcal{O}(10^2)$. In the next section [see discussion below Eq. (62)] we will provide specific numerical examples which make this more evident.

Finally, we come to the phantom phases III.A, III.B. The transition to the phantom phase, which is supposed to be happening during the present cosmological epoch, occurs once ϕ reaches ϕ_0 and μ transitions suddenly to its high value, μ_p. The hidden matter + scalar field energy densities catch up with radiation, start evolving as a phantom fluid with equation of state given by (21), and come to dominate the Universe. The radiation keeps getting diluted as a^{-4} during this phase which we refer to as phase III.A. Since the increase in energy density in the phantom phase

[8]Above we have used a value for $\rho_\gamma^{1/4}(t_{2A})$ of $10^{-3}M_P$, slightly overestimating it. The actual value is typically lower than this, because of the additional Hubble dilution of the energy density of radiation from t_{1A} to t_{2A}. For instance, with the parameters used in the numerical solution for Fig. 1 we have $\rho_\gamma^{1/4}(t_{2A}) \sim 10^{-5}M_p$.

occurs at a very short time scale, all the features of this phase are not very discernible in the log-log plot in Fig. 1, but we have checked them numerically. As we have seen before, the annihilation term will ultimately cause this behavior to transition to a de Sitter phase, when $\Gamma \sim H$ or $\rho_h \sim m^6/M_p^2$. At this point we enter, what we call phase III.B, when all the energy densities become comparable and then tend towards constant values, leading to an asymptotic de Sitter space-time. It is during this phase we expect to generate a scale-invariant spectrum of perturbations. This phase will last until the field ϕ has evolved a distance of $\phi_0 + \phi_R$, when we restart the cycle.

V. NUMBERS AND CONSTRAINTS

So far we have provided general constraints coming from different observations on the couplings and the scales. For the purpose of illustration let us provide some typical values which conform to these constraints and in the process we will also be able to understand the different phases of evolution better. Let us start with the inflationary phase. As already discussed, to obtain the correct amplitude of inflationary fluctuations we will take the reheating to occur at approximately GUT scale energy densities which implies

$$m \sim 10^{-2} M_p. \tag{57}$$

During the course of 60 e-foldings,[9] we find, using Eqs. (33) and (34), that the field ϕ evolves a distance of

$$\Delta\phi_{3B} = 40 M_p \mu_p \xi. \tag{58}$$

As a prototype example, for $\mu_p = 4$ this gives $\Delta\phi_{3B} \sim 200$. This only gives us a constraint on the range when μ is large. For instance, for $\mu_p = 4$ the number of e-foldings during the phantom phase turns out to be [using Eq. (25)] $\Delta\phi_{3A} \sim 30$. To be consistent with inflation we must have $\phi_R \gtrsim 200 + 30 = 230$. Given the fact that these field values are transPlanckian, it is possible that higher order terms in the Lagrangian should not be neglected; we proceed here with the assumption that our starting point is sensible nonetheless.

Depending on the number of e-foldings during the de Sitter phase we find two distinct cases for the spectrum of fluctuations. Case I: If the range of ϕ is such that one gets more than 60 e-foldings of de Sitter, then the CMB fluctuations are scale invariant. As we noted in the Introduction, $n_s \approx 1$ is still consistent with observations [10] once one allows the possibility of running of the tilt and/or tensor modes. If the range in ϕ is such that we have only around 60 e-foldings then the CMB fluctuations at large scales can show a transition from a blue (when the phantom phase will be operating and the reheating mechanism has not kicked in completely) to a scale-invariant spectrum. This could be an interesting and rather unique signature of the model. Case II: If the number of e-foldings in the de Sitter (dS) phase is shorter than 60 e-foldings, the fluctuations that we are observing in the sky must have been generated in the phantom phase. This gives a rather stringent constraint on how far below -1 the phantom equation of state ω_p can be. For a "superinflationary" space-time sourced by phantom fluid, the spectral tilt is expected to be given by

$$\eta_s - 1 = \frac{6(1+\omega_p)}{1+3\omega_p} > 0, \tag{59}$$

implying a blue spectrum. Therefore to be consistent with the observations ω_p has to be very close to -1. For instance, if we include tensor modes, according to [10] at the 2σ level we find

$$\eta_s < 1.01 \Rightarrow \omega_p > -1.01, \tag{60}$$

implying $\mu_p < .581$. This bound is very restrictive, remembering that in order to have a phantom phase we need $\mu_p > 1/\sqrt{3} \approx 0.577$. In the rest of the section we are not going to discuss this possibility any further and concentrate on case I with $\mu_p \gg 1$ which seems more attractive.

Let us next look at the constraint coming from BBN and WMAP on the amount of dark radiation [26]. To be consistent with the data the amount of dark radiation has to be limited to within 10% of ordinary radiation. This essentially imposes a constraint on μ_p, but a rather weak one

$$\mathcal{R}_{\min} < 0.1 \Rightarrow \mu_p \gtrsim 0.17, \tag{61}$$

which is easily satisfied.

What about the range of $\Delta\phi$ during radiation domination? This of course depends on the values of μ_p, μ_r. Just to get an idea, we find for $\mu_p = 4$, $\mu_r = 0.2$, we need

$$\begin{aligned}\Delta\phi &= \Delta\phi_{1A} + \Delta\phi_{1B+2A} + \Delta\phi_{2B} \\ &= \phi_0 - \phi_R \sim 0.70 + 2.16 + 0.66.\end{aligned} \tag{62}$$

As one can see, all the values in the above equation are of the same order of magnitude and therefore no fine-tuning seems to be involved.

Thus the picture that emerges from the above estimates is that for the scenario to work we need relatively longer phases in ϕ when μ is large (58), followed by shorter phases when μ is small. However, the discrepancy in $\Delta\phi$ between Eqs. (58) and (62) is only a few orders of magnitude. Similarly, μ_r and μ_p (in the above example) differ again by only a few orders of magnitude. It is these numbers (the values of $\Delta\phi$ and the two values of μ) that determine the hierarchy between today's meV scale and the GUT scale of inflation via Eq. (56). So we see that,

[9]We choose 60 as a generic typical example for GUT scale inflation; the actual number of e-foldings might be lower or larger than this.

indeed, little fine-tuning is required to explain these disparate mass scales.

Finally, let us come to constraints from dark energy. The main constraint comes from the equation of state parameter. A combined 2σ bound from CMB + BAO + SN is given by $-0.88 > \omega_p > -1.14$ [10]. This provides a constraint on μ_p

$$\mu_p < 0.61. \tag{63}$$

This may seem too small, but we realize that currently we are undergoing the phase transition from small μ to a large μ region, and therefore it is easy to arrange that the ''current'' value of μ satisfies inequality (63) and has not yet reached the constant maximum value μ_p. Equivalently, the equation of state parameter today has not yet reached its late time phantom phase value given by Eq. (21).

VI. CONCLUSIONS

In this paper we have studied a cyclical model of the Universe where the energy density cycles between a minimum value, typically of the order of meV^4 and a maximum value roughly set by the GUT scale. This effectively provides a connection between the current accelerated expansion we observe today and the inflationary era in the past. The scale factor continues to grow from one cycle to the next (there is no ''turnaround''). In order to achieve this model we postulated the existence of some ''hidden'' sector matter coupled to a ghostlike scalar field. This mechanism is responsible for a superaccelerated phantom expansion. Allowing for hidden sector particles to be converted to light degrees of freedom of the standard model ameliorates the phantom behavior, effectively transitioning to a de Sitter-like expansion, therefore avoiding the big-rip singularity. Although dominated by radiation, in this phase all the energy densities remain constant. Therefore, if most of the cosmological perturbations are generated during this exponential inflationary era, the spectrum is expected to be scale invariant. Even if not favored by the data, this is still a possibility. Another possibility would be to have some of the fluctuations generated during the phantom phase which will show up as a blue tilt in the spectrum. In that case we will see a running of the tilt which could be a unique possible signature of the model.

In order to achieve the cyclic behavior, we have postulated that the coupling between the ghost scalar field and the hidden sector is constant piecewise. This procedure might seem *ad hoc*, but it is just the simplest possibility. We found that no fine-tuning seems to be involved when requiring one to have a long enough radiation/matter dominated phase. It is also worth mentioning that the smallness problem associated with dark energy is circumvented. The only parameter we need in order to describe the current acceleration is the coupling between the hidden sector and the ghost field, and it has a value not much greater than 1.

ACKNOWLEDGMENTS

T. B. would like to acknowledge the hospitality of the physics department at the University of Minnesota at Minneapolis. K. F. and C. I. are supported by the U.S. Department of Energy and MCTP via the University of Michigan.

APPENDIX: A STABILITY OF SCALING SOLUTIONS IN PHANTOM COUPLED MODELS

We will look at ghost fields coupled to radiation or matter via the term $\rho_\gamma = \tilde{\rho}_\gamma \epsilon^{2\mu\phi}$ and study the stability of the critical points, generalizing the analysis done in [27]. In this way we will find the stable attractors and conditions necessary to obtain them. Here the subscript γ refers to the adiabatic index of the fluid the phantom field couples to, defined as $\gamma = 1 + \omega_h$. Throughout the main body of the paper we have used ρ_h, but for notational convenience here we will replace it by ρ_γ. It will be assumed that the phantom field has a self-interaction potential of the following forms: $V(\phi) = V_0 \epsilon^{-2\alpha\phi}$ and $V(\phi) = -V_0 \epsilon^{2\alpha\phi}$. We have not used a potential in deriving our main results in the paper, but we keep it here for generality and further reference.

For

$$V(\phi) = V_0 e^{-2\alpha\phi} \tag{A1}$$

we have the following equations:

$$\ddot{\phi} + 3H\dot{\phi} = V_{\text{eff}}(\phi)' \qquad \dot{H} = -\frac{1}{2}(-\dot{\phi}^2 + \gamma\tilde{\rho}_\gamma \epsilon^{2\mu\phi})$$
$$H^2 = \frac{1}{3}\left[-\frac{\dot{\phi}^2}{2} + V(\phi) + \tilde{\rho}_\gamma \epsilon^{2\mu\phi}\right], \tag{A2}$$

where $V_{\text{eff}} = V(\phi) + \tilde{\rho}_\gamma \epsilon^{2\mu\phi}$. Although we are treating here only two fluids, this case is relevant during the phantom phase, when the energy density of any (third) component not coupled to the phantom field, such as regular matter, will quickly become subdominant. Introducing the variables

$$x = \frac{\dot{\phi}}{\sqrt{6}H} \tag{A3}$$

and

$$y = \frac{\sqrt{V(\phi)}}{\sqrt{3}H} \tag{A4}$$

and using $\eta \equiv \log a(t)$ as the independent variable, instead of the cosmological time t, we can rewrite the equations in the form of an autonomous system supplemented with the Hubble constraint,

$$\begin{aligned} x' &= -3x + \sqrt{6}[\mu(1 + x^2 - y^2) - \alpha y^2] \\ &\quad + \tfrac{3}{2}x[\gamma(1 + x^2 - y^2) - 2x^2], \\ y' &= -\sqrt{6}\alpha xy + \tfrac{3}{2}y[\gamma(1 + x^2 - y^2) - 2x^2], \\ 1 &= [y^2 - x^2 + \Omega_\gamma]. \end{aligned} \tag{A5}$$

In order to find the critical points one has to set the rhs of the first two equations to zero and solve for x and y. We find five distinct solutions,

$$(x, y) = \begin{cases} (i, 0) & I. \\ (-i, 0) & II. \\ (-\frac{2}{3}\frac{\sqrt{6}\mu}{-2+\gamma}, 0) & III. \\ (\frac{1}{4}\frac{\sqrt{6}\gamma}{\alpha+\mu}, \frac{1}{4}\frac{\sqrt{2}\sqrt{8\mu\alpha+8\mu^2-6\gamma+3\gamma^2}}{\alpha+\mu}) & IV. \\ (-\frac{1}{3}\sqrt{6}\alpha, -\frac{1}{3}\sqrt{3}\sqrt{3+2\alpha^2}) & V. \end{cases}$$

Note that the first two are nonphysical so we will no longer consider them. Next we compute the fractional densities for the phantom field and its adiabatic constant near the five critical points. The Hubble constraint will then enforce additional existence conditions,

$$\Omega_\phi = y^2 - x^2 = \begin{cases} -\frac{8}{3}\frac{\mu^2}{(-2+\gamma)^2} & III. \\ -\frac{1}{4}\frac{-4\mu\alpha-4\mu^2+3\gamma}{(\alpha+\mu)^2} & IV. \\ 1 & V. \end{cases} \tag{A6}$$

One solution is completely dominated by the scalar field ϕ and the other two exhibit a scaling behavior. For the first of those, the Hubble constraint will not give any additional inequalities in the parameter space since $\Omega_{\phi(III.)}$ is clearly negative, hence less than 1. Here the roman numeral subscript refers to all the solutions, including the nonphysical ones, i.e., $(I.)$ corresponds to the solutions with $(x, y) = (i, 0)$ and so on. Also, $\Omega_{\phi(IV)} < 1$ is trivially satisfied for positive parameters. Thus, the only nontrivial existence constraint comes from imposing reality of the $y_{IV.}$ solution:

$$\mu(\mu + \alpha) \geq \tfrac{3}{8}\gamma(2 - \gamma). \tag{A7}$$

Let us now look at the ''effective'' values of the adiabatic constant $\gamma = 1 + w$ for the ghost field near the critical points. For completeness we will keep even the nonphysical solutions,

$$\gamma_\phi = 1 + \frac{p_\phi}{\rho_\phi} = \frac{\dot\phi^2}{\frac{1}{2}\dot\phi^2 - V(\phi)} = \frac{2x^2}{x^2 + y^2}. \tag{A8}$$

With this definition we get

$$\gamma_\phi = \frac{2x^2}{-y^2 + x^2} = \begin{cases} 2 & I. \\ 2 & II. \\ 2 & III. \\ -\frac{3\gamma^2}{-4\mu\alpha-4\mu^2+3\gamma} & IV. \\ -\frac{4}{3}\alpha^2 & V. \end{cases} \tag{A9}$$

The total, or effective DE equation of state parameter that drives the expansion can be defined since we have scaling solutions,

$$\omega_{\text{tot}} = \frac{p_\phi + p_\gamma}{\rho_\phi + \rho_\gamma}. \tag{A10}$$

Some algebra leads to

$$\omega_{\text{tot}} = \Omega_\phi(\gamma_\phi - 1) + (1 - \Omega_\phi)(\gamma - 1). \tag{A11}$$

For the three physical solutions it leads to the following values:

$$\omega_{\text{tot}} = \begin{cases} \frac{1}{3}\frac{3\omega_h(\omega_h-1)+8\mu^2}{\omega_h-1} & III. \\ \frac{1}{2}\frac{3(1+\omega_h)^2+2(\mu+\alpha)(\omega_h\alpha-\mu)}{(\alpha+\mu)^2} & IV. \\ -1 - \frac{4}{3}\alpha^2 & V. \end{cases} \tag{A12}$$

Next we will study the stability of the relevant critical points, ignoring the nonphysical first two solutions. The technique is the following. One expands around the critical solution setting $x = x_c + u$ and $y = y_c + v$ into (A5) and then keeps only linear terms. In order to have a stable solution the eigenvalues of the matrix describing the linearized system must have negative real parts. For solution $III.$, one finds the following equations:

$$\begin{aligned} u' &= -\frac{1}{2}\frac{-8\mu^2 - 3\gamma^2 + 12\gamma - 12}{-2 + \gamma}u, \\ v' &= -\frac{1}{2}\frac{(-3\gamma^2 - 8\mu\alpha - 8\mu^2 + 6\gamma)}{-2 + \gamma}v. \end{aligned} \tag{A13}$$

For both radiation ($\gamma = \frac{4}{3}$) and dust ($\gamma = 1$) the coefficient u is negative independent of the value of μ. From the second equation one gets that the node is stable when

$$3\gamma(2 - \gamma) < 8\mu(\alpha + \mu). \tag{A14}$$

Otherwise we have a saddle point. It is interesting to notice that this is exactly the same condition we got in (A7) for the existence of the fourth solution.

Let us move on to the stability of solution IV, for which the linearized system becomes

$$u' = -\frac{1}{8}\frac{24\alpha^2 - 24\gamma\mu^2 + 24\mu^2 + 48\mu\alpha + 18\gamma^2 - 36\gamma\alpha\mu - 9\gamma^3 - 12\gamma\alpha^2}{(\mu+\alpha)^2}u$$
$$-\frac{1}{8}\frac{\sqrt{3}\sqrt{8\mu\alpha + 8\mu^2 - 6\gamma + 3\gamma^2}(16\mu\alpha + 3\gamma^2 + 8\mu^2 + 8\alpha^2)}{(\alpha+\mu)^2}v, \quad \text{(A15)}$$
$$v' = \frac{1}{8}\frac{\sqrt{3}\sqrt{8\mu\alpha + 8\mu^2 - 6\gamma + 3\gamma^2}(-4\alpha^2 + 3\gamma^2 - 4\mu\alpha - 6\gamma)}{(\alpha+\mu)^2}u - \frac{3}{8}\frac{\gamma(8\mu\alpha + 8\mu^2 - 6\gamma + 3\gamma^2)}{(\alpha+\mu)^2}v.$$

The eigenvalues are

$$e_{1(4)} = \frac{1}{4}\frac{1}{\alpha+\mu}(3\alpha\gamma - 6\alpha - 6\mu + B^{1/2}),$$
$$e_{2(4)} = \frac{1}{4}\frac{1}{\alpha+\mu}(3\alpha\gamma - 6\alpha - 6\mu - B^{1/2}), \quad \text{(A16)}$$

where B is the following combination of the parameters:

$$B = 72\mu\alpha(\gamma^2 + 1 + \tfrac{8}{3}(\mu+\alpha)^2) + 54\gamma^2(\gamma - 2)$$
$$+ \alpha^2(36 + 81\gamma^2 - 180\gamma) + 36\gamma(\gamma - \alpha\mu + 4\mu^2).$$

The study of stability of the solutions is quite complicated here but there is a range of parameters for which the real part of the two eigenvalues is negative. Independent of the value of B one necessary condition for stability here is

$$2\left(1 + \frac{\mu}{\alpha}\right) < \gamma. \quad \text{(A17)}$$

For positive parameters, and if γ is either 1 or $\frac{4}{3}$ this inequality cannot be satisfied; thus the fourth attractor is unstable if the hidden sector is comprised of some component that behaves like matter or radiation.

Let us look now at the stability conditions for the critical point labeled by *V*. The linearized autonomous system becomes in this case:

$$u' = (-3 + 2\alpha^2(\gamma - 3) - 4\mu\alpha)u$$
$$+ \sqrt{2}\sqrt{3 + 2\alpha^2}(2\mu - \alpha\gamma + 2\alpha)v, \quad \text{(A18)}$$
$$v' = \sqrt{2}\sqrt{3 + 2\alpha^2}(\alpha\gamma - \alpha)u - \gamma(3 - 2\alpha^2)v.$$

The eigenvalues read $-(3 + 2\alpha^2)$ and $-(4\alpha^2 + 4\mu\alpha + 3\gamma)$ which are clearly both negative and real so one has a stable node as a late time attractor. Also remember that this solution does not have a scaling behavior, since in this case the energy density is dominated by the phantom. In conclusion we found two stable late time attractors, one of which exhibits a scaling behavior. Notice also that this scaling solution corresponds to a critical point where $y = 0$, so in effect it is equivalent to the case where the potential is actually zero.

Next let us look at the tracking ratio in the two cases of interest, namely, the third and fourth critical points. The tracking ratio is defined to be the ratio of relic densities of the two components,

$$r = \frac{\Omega_\phi}{1 - \Omega_\phi}. \quad \text{(A19)}$$

With this definition we find, using (A6):

$$r = \begin{cases} -\frac{8}{3}\frac{\mu^2}{(-2+\gamma)^2(1+\frac{8}{3}\frac{\mu^2}{(-2+\gamma)^2})} & III. \\ -\frac{1}{4}\frac{-4\mu\alpha - 4\mu^2 + 3\gamma}{(\mu+\alpha)^2(1+\frac{1}{4}\frac{-4\mu\alpha-4\mu^2+3\gamma}{(\mu+\alpha)^2})} & IV. \end{cases}$$

Since we have established that we will be using the late time attractor described by critical point *III*. as our model for the phantom phase, let us actually see under what conditions we cross the ''phantom divide'' and if this phase will be stable. Comparing $\omega_{\rm tot}$ given by (A12) to -1 we find the following restriction on μ:

$$\mu^2 \geq \begin{cases} \frac{3}{8} & \text{for matter hidden sector} \\ \frac{1}{3} & \text{for radiation hidden sector} \end{cases}. \quad \text{(A20)}$$

Looking back at (A14) and taking $\alpha = 0$ as appropriate for the case of no potential one can check that the stability conditions are actually identical with the conditions for achieving a phantom phase, listed above. Hence, we have verified that the late time attractor solution for $V(\phi) = 0$ is stable once we have μ such that we get a phantom phase.

Now for generality we will repeat the same analysis for a negative potential,

$$V(\phi) = -V_0 \exp 2\alpha\phi. \quad \text{(A21)}$$

Here we will define $y = \frac{\sqrt{-V(\phi)}}{\sqrt{3}H}$. In this case the autonomous system will take the following form:

$$x' = -3x + \sqrt{6}[\mu(1 + x^2 + y^2) - \alpha y^2]$$
$$+ \tfrac{3}{2}x[\gamma(1 + x^2 + y^2) - 2x^2],$$
$$y' = \sqrt{6}\alpha xy + \tfrac{3}{2}y[\gamma(1 + x^2 + y^2) - 2x^2], \quad \text{(A22)}$$
$$1 = [-y^2 - x^2 + \Omega_\gamma].$$

There will be only two physical critical points in this case:

$$(x, y) = \begin{cases} (-\frac{2}{3}\frac{\sqrt{6}\mu}{-2+\gamma}, 0) & I.B \\ (\frac{1}{4}\frac{\sqrt{6}\gamma}{-\alpha+\mu}, \frac{1}{4}\frac{\sqrt{2}\sqrt{8\mu\alpha - 8\mu^2 + 6\gamma - 3\gamma^2}}{-\alpha+\mu}) & II.B \end{cases}.$$

Just to clear any possible confusion, please note that the labels *I.B* and *II.B* here are not related to the labeling of the different regions in Fig. 1. Notice that the first critical point

in this case is identical to the third critical point for the case of positive potential [see the equation below (A5)]. The existence condition for the second critical point reads $\mu(\mu-\alpha)<\frac{3}{8}\gamma(2-\gamma)$. Fractional density values are

$$\Omega_\phi = -y^2 - x^2 = \begin{cases} -\frac{8}{3}\frac{\mu^2}{(-2+\gamma)^2} & I.B \\ \frac{1}{4}\frac{-4\mu\alpha+4\mu^2-3\gamma}{(-\alpha+\mu)^2} & II.B \end{cases}. \tag{A23}$$

From here we get an additional existence constraint on the second critical point, namely:

$$\alpha(\mu-\alpha) \le \frac{3}{4}\gamma. \tag{A24}$$

The adiabatic constant for ϕ is

$$\gamma_\phi = \frac{2x^2}{y^2+x^2} = \begin{cases} 2 & I.B \\ -\frac{3\gamma^2}{-4\mu\alpha+4\mu^2-3\gamma} & II.B \end{cases}. \tag{A25}$$

Notice the difference between the last value in (A25) and the fourth in (A9). Here we can set $\mu \to 0$ and recover γ as the adiabatic index. Before the naive limit was $-\gamma$ but one was not actually allowed to take that limit due to (A7). Now the inequality has been reversed so the second critical point in the case of the negative potential could be used for a scaling solution in a phase where the hidden sector decouples from the ghost field.

As before let us look at the effective equation of state parameter:

$$\omega_{\rm tot} = \begin{cases} \frac{1}{3}\frac{3\omega_h(\omega_h-1)+8\mu^2}{\omega_h-1} & I.B \\ \frac{\omega_h\alpha+\mu}{\alpha-\mu} & II.B \end{cases}. \tag{A26}$$

Expanding around the critical points for the first solution we get the following conditions for stability:

$$\begin{aligned} 0 &> -\frac{1}{2}\frac{-8\mu^2-3\gamma^2+12\gamma-12}{-2+\gamma}, \\ 0 &> -\frac{1}{2}\frac{(-3\gamma^2+8\mu\alpha-8\mu^2+6\gamma)}{-2+\gamma}. \end{aligned} \tag{A27}$$

The first inequality is trivially satisfied and the second implies

$$\gamma(2-\gamma) < \frac{8}{3}\mu(\mu-\alpha). \tag{A28}$$

This could be used as a constraint on the steepness of the potential in order to preserve the tracking behavior in the phantom phase. For the second critical point we have the following eigenvalues:

$$\begin{aligned} e_{1(2)} &= \frac{1}{4}\frac{1}{\alpha-\mu}(3\alpha\gamma-6\alpha+6\mu+B_2^{1/2}), \\ e_{2(2)} &= \frac{1}{4}\frac{1}{\alpha-\mu}(3\alpha\gamma-6\alpha+6\mu-B_2^{1/2}). \end{aligned} \tag{A29}$$

Here B_2 is a combination of the parameters, the exact form of which we will not be using. A necessary condition for the stability of this critical point is

$$\alpha(1-\omega_h) < 2\mu. \tag{A30}$$

The tracking ratios can be easily computed:

$$r = \begin{cases} -\frac{8}{3}\frac{\mu^2}{(-2+\gamma)^2(1+\frac{8}{3}\frac{\mu^2}{(-2+\gamma)^2})} & I.B \\ -\frac{-4\mu\alpha+4\mu^2-3\gamma}{-4\alpha^2+4\alpha\mu-3\gamma} & II.B \end{cases}.$$

In this Appendix, we have found the conditions for scaling behavior in the phantom phase, for the cases of positive, zero, and negative exponential potentials. An exponential coupling between a ghostlike field and some hidden sector fluid is used to generate a phantom phase, where the effective equation of state is less than negative 1. We found the stable attractors and conditions necessary to obtain them. As a side result we notice that for negative potentials one could have a scaling stable late time attractor even if the ghost field is decoupled from the hidden sector. In that case the ghost will just track the hidden sector component.

APPENDIX: B ESTIMATING THE MINIMUM VALUE OF $\mathcal{R}$

Here we will estimate the minimum value of the ratio between the hidden sector energy density and the radiation energy density

$$\mathcal{R} \equiv \frac{\rho_h}{\rho_\gamma}, \tag{B1}$$

during the reheating phase (see Fig. 1 regions *I.A* and *I.B*). Once we enter the transition phase (region *I.A*), if μ is large enough, most of the energy density will be stored in radiation, followed by the phantom field, and the least amount is contained by the hidden matter sector. To a good approximation we will use "radiation domination" in what follows, since we are only interested in order of magnitude estimates.

First we will look at the case when the hidden matter is nonrelativistic when this transition occurs, i.e., $\omega = 0$. Setting μ_r to zero, as appropriate for the transition to radiation, we will have the following equations for the evolution of the system:

$$\dot\rho_h + 3H\rho_h = -\rho_h\Gamma, \tag{B2}$$

$$\ddot\phi + 3H\dot\phi = 0, \tag{B3}$$

$$\dot\rho_\gamma + 4H\rho_\gamma = 0, \tag{B4}$$

along with the Hubble equation

$$H^2 = \frac{1}{3M_p^2}(\rho_\gamma). \tag{B5}$$

We have neglected the annihilation term in Eq. (B4) because $\rho_h\Gamma \ll 4H\rho_\gamma$ will be satisfied very quickly after the

transition from the de Sitter phase is started. The solutions for the energy densities are simple:

$$\rho_h(t) = \frac{1}{t^{3/2}C_1 - 2tm^{-3}}, \tag{B6}$$

$$\rho_\gamma(t) = \frac{3M_p^2}{4t^2}, \tag{B7}$$

where C_1 is an integration constant we still have to fix. We have used the fact that during radiation domination $H \sim 1/2t$ in order to get the coefficient for the radiation energy density. Since it takes a longer time for the annihilation term to be subdominant with respect to the Hubble dampening term in the hidden matter continuity equation, we will have a short period where the energy density in hidden matter is decreasing faster than a^{-3}. This yields a minimum value for the parameter $\mathcal{R}$. Simply setting $\dot{\mathcal{R}}(t) = 0$ leads to $\Gamma(t_c) \sim H(t_c)$. In order to fix the integration constant C_1, we need to know at what time we start the transition from the de Sitter to the radiation dominated phase. Using the initial condition[10] in (35) along with Eq. (B7), the transition time is found to be

$$t_{1A} = \left(\frac{3M_p^4\xi}{m^6\eta^3}\right)^{1/2}. \tag{B8}$$

Furthermore, C_1 is obtained by requiring that the hidden matter density ρ_h value in the de Sitter phase matches the value estimated at the transition time t_{1A}, obtained from (B6). The initial conditions (33) together with (32) allow us to evaluate the initial value of hidden matter density at the beginning of the transition phase. In the limit of $\mu_p \gg 1$ we get the following simplified form for the integration constant:

$$C_1 = \frac{\sqrt{3}(3M_p^2 + 32\sqrt{3}\mu_p^3 m^3 t_{1A})}{48m^6\mu_p^3 t_{1A}^{3/2}}. \tag{B9}$$

In order to get the minimum value for $\mathcal{R}$ we go back to the condition $\Gamma = \frac{\rho_h(t_c)}{m^3} \sim H(t_c)$, where t_c represents the time at which this minimum is attained. This can be rewritten as

$$\frac{\rho_h}{m^3} \sim \frac{\rho_\gamma^{1/2}}{\sqrt{3}M_p}, \tag{B10}$$

leading to

$$R_{\min} \sim \frac{2m^3 t_c}{3M_p^2}. \tag{B11}$$

[10]Here we consider the transition from the dS phase to the radiation dominated phase due to the sudden drop in the coupling between the hidden sector fields and the ghost field. The asymptotic value (valid for the dS phase) for the energy density in the rhs of Eq. (35) here becomes an initial condition for the transition phase, region *I*..

Also, from (B10) we can solve for t_c using (B6) and (B7): $t_c = \frac{16}{C_1^2 m^6}$. Plugging into (B11) we get the simplified form:

$$\mathcal{R}_{\min} = \frac{32}{3M_p^2 m^3 C_1^2}. \tag{B12}$$

Using (B8) and (B9) in the above equation we obtain the final result, expressed only in terms of μ_p:

$$\mathcal{R}_{\min} = \frac{16}{\sqrt{3}\mu_p^{3/2}(1 + 4\sqrt{\mu_p})^2}. \tag{B13}$$

Let us now turn our attention to the case where the hidden matter becomes relativistic at the energy scales where the transition between the de Sitter and the radiation phases occurs. At the beginning there will still be a regime where the annihilation is effective, thus lowering the value of the ratio between the hidden matter energy density and the radiation energy density. If $\mu_r = 0$, instead of a minimum we will now have a constant asymptotic value towards which this ratio will tend. This is due to the fact that once the conversion is no longer efficient, both hidden matter and radiation energy densities will scale as a^{-4}. For completeness and generality we will study the case where $\mu_r \neq 0$. As we shall shortly see here a minimum develops, just as we have seen in the case of nonrelativistic hidden matter. The approximative equations we need to solve are

$$\dot{\rho}_h + 4H\rho_h = -\rho_h\Gamma + 2\rho_h\dot{\phi}\frac{\mu_r}{M_p}, \tag{B14}$$

$$\ddot{\phi} + 3H\dot{\phi} = 0, \tag{B15}$$

$$\dot{\rho}_\gamma + 4H\rho_\gamma = 0, \tag{B16}$$

along with the Hubble equation

$$H^2 = \frac{1}{3M_p^2}\rho_\gamma. \tag{B17}$$

Notice that we have neglected the ρ_h terms in the second and third equations since we are interested in the phase of rapid conversion of hidden sector particles to radiation. Therefore, in this regime the energy density stored in the hidden sector will decay much faster than a^{-4}. Essentially the reason for this being that μ has transitioned from large to small values, i.e., $\mu_p \gg \mu_r$. The system admits the following solutions:

$$H(t) = \frac{1}{2t}, \tag{B18}$$

$$\rho_\gamma(t) = \frac{3M_p^2}{4t^2}, \tag{B19}$$

$$\dot{\phi}(t) = \frac{A_\phi}{t^{3/2}}, \tag{B20}$$

$$\rho_h(t) = \frac{8m^3 {A_\phi}^2 {\mu_r}^2}{D(t)}, \tag{B21}$$

where $D(t)$ is

$$D(t) = 4t^{3/2} M_p A_\phi \mu_r + t^2 {M_p}^2 + 8t^2 e^{4(A_\phi \mu_r / M_p \sqrt{t})} C_h m^3 {A_\phi}^2 {\mu_r}^2.$$

In order to obtain the integration constants C_h and A_ϕ we match the energy densities above, evaluated at the transition time t_{1A} with the corresponding values from the de Sitter phase, given in (32)–(35). As before, t_{1A} is given by (B8). For A_ϕ this leads to

$$A_\phi = \frac{2}{3} \frac{\mu_p {M_p}^2 3^{3/4} \xi^{3/4}}{\eta^{5/4} m^{3/2}}. \tag{B22}$$

The expression for C_h for general μ_p turns out to be messy, but it can be simplified in the limit $\mu_p \gg 1$ to

$$C_h = -\frac{1}{3} \frac{\sqrt{3}\mu_p(-4\mu_r^2 + 4\mu_p\mu_r + \mu_p) e^{-4\mu_r}}{{M_p}^2 {\mu_r}^2}. \tag{B23}$$

Above we have used $\xi \sim \frac{3\sqrt{3}}{\mu_p}$ and $\eta \sim 4\sqrt{3}\mu_p$, expressions valid in the $\mu_p \gg 1$ limit.

Since we have $\mu_r \neq 0$, we expect a minimum of the ratio $\mathcal{R}$ to develop. Reexpressing $\dot{\mathcal{R}} = 0$ by use of the definition of $\mathcal{R}$, the ratio between the hidden sector and the radiation energy densities, and of Eqs. (B14) and (B15) we get

$$\Gamma(\rho_h + \rho_r) = 2\rho_r \dot{\phi} \frac{\mu_r}{M_p}. \tag{B24}$$

Defining t_c the time at which the above equation holds, we find that

$$\mathcal{R}_{\min} \sim \frac{2m^3 \dot{\phi}(t_c)\mu_r}{M_p \rho_\gamma(t_c)} = \frac{8}{3} \frac{m^3 \mu_r A_\phi \sqrt{t_c}}{{M_p}^3}. \tag{B25}$$

From (B24) we can also obtain t_c by using the solutions we have for the energy densities in (B19) and (B21). In order to get a closed form we will need to do some approximation of the exponent in the denominator of (B21). Since $t > t_{1A}$ we can show using t_{1A} from (B8) and A_ϕ from (B22) that $\frac{4A_\phi \mu_r}{M_p \sqrt{t}} \leq 4\mu_r$. Since $\mu_r \ll 1$ we will truncate the expansion of the exponential at terms of $\mathcal{O}(\mu_r^2)$, leading to

$$t_c = 1024 \frac{{C_h}^2 m^6 {A_\phi}^6 {\mu_r}^6}{{M_p}^2 ({M_p}^2 + 8C_h m^3 {A_\phi}^2 {\mu_r}^2)^2}. \tag{B26}$$

Going back to (B25) we get, after some algebra, the following form for $\mathcal{R}_{\min}$:

$$\mathcal{R}_{\min} = \frac{4}{\sqrt{3}} \frac{{\mu_r}^2}{{\mu_p}^2} e^{-4\mu_r} \times \left| \frac{1}{e^{-4\mu_r} - \mu_p(\mu_p + 4\mu_r(\mu_p - \mu_r))^{-1}} \right|.$$

We can double expand this expression in μ_r and μ_p^{-1} and keep only the leading terms:

$$\mathcal{R}_{\min} \sim \frac{1}{18} \frac{\sqrt{3}(3 + 8\mu_r)}{\mu_p^2} + \mathcal{O}(\mu_r^2, \mu_p^{-3}). \tag{B27}$$

In the limit $\mu_r \to 0$ we get the result in Eq. (41).

[1] S. Alexander, T. Biswas, A. Notari, and D. Vaid, arXiv:0712.0370.

[2] T. Biswas, R. Mansouri, and A. Notari, J. Cosmol. Astropart. Phys. 12 (2007) 017.

[3] M. N. Celerier, arXiv:astro-ph/0702416.

[4] P. J. E. Peebles and B. Ratra, Rev. Mod. Phys. **75**, 559 (2003).

[5] R. R. Caldwell and M. Kamionkowski, arXiv:0903.0866.

[6] A. Silvestri and M. Trodden, Rep. Prog. Phys. **72**, 096901 (2009).

[7] R. R. Caldwell, Phys. Lett. B **545**, 23 (2002); A. E. Schulz and M. J. White, Phys. Rev. D **64**, 043514 (2001); R. R. Caldwell, M. Kamionkowski, and N. N. Weinberg, Phys. Rev. Lett. **91**, 071301 (2003); J. G. Hao and X. Z. Li, Phys. Rev. D **67**, 107303 (2003); G. W. Gibbons, arXiv:hep-th/0302199; S. Nojiri and S. D. Odintsov, Phys. Lett. B **562**, 147 (2003); P. Singh, M. Sami, and N. Dadhich, Phys. Rev. D **68**, 023522 (2003); M. P. Dabrowski, T. Stachowiak, and M. Szydlowski, Phys. Rev. D **68**, 103519 (2003); J. G. Hao and X. Z. Li, Phys. Rev. D **70**, 043529 (2004); V. B. Johri, Phys. Rev. D **70**, 041303 (2004); U. Alam, V. Sahni, T. D. Saini, and A. A. Starobinsky, Mon. Not. R. Astron. Soc. **354**, 275 (2004); M. Sami and A. Toporensky, Mod. Phys. Lett. A **19**, 1509 (2004); B. Feng, X. L. Wang, and X. M. Zhang, Phys. Lett. B **607**, 35 (2005); Z. K. Guo, Y. S. Piao, X. M. Zhang, and Y. Z. Zhang, Phys. Lett. B **608**, 177 (2005); I. Y. Aref'eva, A. S. Koshelev, and S. Y. Vernov, Phys. Rev. D **72**, 064017 (2005); B. Feng, M. Li, Y. S. Piao, and X. Zhang, Phys. Lett. B **634**, 101 (2006); Y. S. Piao and E. Zhou, Phys. Rev. D **68**, 083515 (2003); Y. S. Piao and Y. Z. Zhang, Phys. Rev. D **70**, 063513 (2004).

[8] M. G. Brown, K. Freese, and W. H. Kinney, J. Cosmol. Astropart. Phys. 08 (2008) 002.

[9] S. Nojiri and S. D. Odintsov, arXiv:0807.0685; G. Cognola, E. Elizalde, S. D. Odintsov, P. Tretyakov, and S. Zerbini, Phys. Rev. D **79**, 044001 (2009); G. Cognola *et al.*, Phys. Rev. D **77**, 046009 (2008); G. Barenboim and

J. D. Lykken, Phys. Lett. B **633**, 453 (2006).
[10] E. Komatsu *et al.* (WMAP Collaboration), Astrophys. J. Suppl. Ser. **180**, 330 (2009).
[11] P. Creminelli, M. A. Luty, A. Nicolis, and L. Senatore, J. High Energy Phys. 12 (2006) 080;
[12] N. Arkani-Hamed, H. C. Cheng, M. A. Luty, and S. Mukohyama, J. High Energy Phys. 05 (2004) 074.
[13] R. Bean, E. E. Flanagan, and M. Trodden, Phys. Rev. D **78**, 023009 (2008).
[14] R. Bean, E. E. Flanagan, I. Laszlo, and M. Trodden, Phys. Rev. D **78**, 123514 (2008).
[15] T. Biswas and A. Mazumdar, arXiv:hep-th/0408026; Phys. Lett. B **634**, 437 (2006); T. Biswas, R. Brandenberger, A. Mazumdar, and T. Multamaki, Phys. Rev. D **74**, 063501 (2006).
[16] L. Amendola, Phys. Rev. D **62**, 043511 (2000); L. Amendola and C. Quercellini, Phys. Rev. D **68**, 023514 (2003); L. Amendola and D. Tocchini-Valentini, Phys. Rev. D **64**, 043509 (2001); L. Amendola, M. Gasperini, and F. Piazza, J. Cosmol. Astropart. Phys. 09 (2004) 014.
[17] S. M. Carroll, M. Hoffman, and M. Trodden, Phys. Rev. D **68**, 023509 (2003); J. M. Cline, S. Jeon, and G. D. Moore, Phys. Rev. D **70**, 043543 (2004).
[18] N. Moeller and B. Zwiebach, J. High Energy Phys. 10 (2002) 034; N. Barnaby, T. Biswas, and J. M. Cline, J. High Energy Phys. 04 (2007) 056; I. Y. Aref'eva, L. V. Joukovskaya, and S. Y. Vernov, J. High Energy Phys. 07 (2007) 087; I. Y. Aref'eva, AIP Conf. Proc. **957**, 297 (2007).
[19] T. D. Lee and G. C. Wick, Nucl. Phys. **B9**, 209 (1969); Phys. Rev. D **2**, 1033 (1970); B. Grinstein, D. O'Connell, and M. B. Wise, Phys. Rev. D **77**, 025012 (2008); A. van Tonder, arXiv:0810.1928; A. M. Shalaby, Phys. Rev. D **80**, 025006 (2009); S. Lee, arXiv:0810.1145.
[20] J. D. Barrow and C. G. Tsagas, Classical Quantum Gravity **26**, 195003 (2009); S. Dubovsky, T. Gregoire, A. Nicolis, and R. Rattazzi, J. High Energy Phys. 03 (2006) 025; V. A. Rubakov, Theor. Math. Phys. **149**, 1651 (2006); P. Creminelli, G. D'Amico, J. Norena, and F. Vernizzi, J. Cosmol. Astropart. Phys. 09 (2009) 018; J. Sadeghi, M. R. Setare, and A. Banijamali, Phys. Lett. B **678**, 164 (2009); M. Libanov, V. Rubakov, E. Papantonopoulos, M. Sami, and S. Tsujikawa, J. Cosmol. Astropart. Phys. 07 (2007) 010.
[21] T. Biswas, arXiv:0801.1315; T. Biswas and S. Alexander, Phys. Rev. D **80**, 043511 (2009); T. Biswas and A. Mazumdar, Phys. Rev. D **80**, 023519 (2009).
[22] Y. F. Cai, T. Qiu, Y. S. Piao, M. Li, and X. Zhang, J. High Energy Phys. 10 (2007) 071.
[23] J. E. Lidsey, D. J. Mulryne, N. J. Nunes, and R. Tavakol, Phys. Rev. D **70**, 063521 (2004); D. J. Mulryne, N. J. Nunes, R. Tavakol, and J. E. Lidsey, Int. J. Mod. Phys. A **20**, 2347 (2005); D. J. Mulryne, R. Tavakol, J. E. Lidsey, and G. F. R. Ellis, Phys. Rev. D **71**, 123512 (2005); J. Khoury, B. A. Ovrut, P. J. Steinhardt, and N. Turok, arXiv: hep-th/0105212; Phys. Rev. D **66**, 046005 (2002).
[24] R. Tolman, *Relativity, Thermodynamics, and Cosmology* (Oxford, Claredon, 1934).
[25] P. J. Steinhardt and N. Turok, New Astron. Rev. **49**, 43 (2005); Science **296**, 1436 (2002); Phys. Rev. D **65**, 126003 (2002).
[26] K. Ichiki, M. Yahiro, T. Kajino, M. Orito, and G. J. Mathews, Phys. Rev. D **66**, 043521 (2002); K. A. Olive, G. Steigman, and T. P. Walker, Phys. Rep. **333**, 389 (2000).
[27] E. J. Copeland, A. R. Liddle, and D. Wands, Phys. Rev. D **57**, 4686 (1998).